

# Effect of Seed Size on Crystallization Behavior of MPP0

Yoshitaka Nakata,<sup>\*,†</sup> Youko Kiyosawa,<sup>†</sup> Kooji Kagara,<sup>†</sup> and Masakuni Matsuoka<sup>‡</sup>

OHARA Pharmaceutical Co., Ltd., 121-15, Toriino, Koka-cho, Koka-shi, Shiga 520-3403, Japan, and Tokyo University of Agriculture and Technology, 2-24-16, Nakacho, Koganei-shi, Tokyo 184-8588, Japan

## Abstract:

Based on our recent study on the batch crystallization of polymorphic mixture of 4-(1-(2-(3-methoxyphenethyl)phenoxy)-3-(dimethylamino)propan-2-yloxy)-4-oxobutanoic acid (MPP0), in which the polymorphic composition was found to vary with the seed composition and with the seeding temperature, and size-dependent compositions were also observed, particle size and composition distributions were measured to clarify these phenomena. The polymorphic composition of the product varied with seed size, and it was always lower than the seed composition. From the size and polymorphic distributions, as well as volume shape factors, the crystallization behaviors of the two polymorphs (Form A and Form B) were discussed, and we concluded that Form B grows faster and nucleates more easily than Form A.

## 1. Introduction

Seeding methods are effective for producing desired polymorphs. To enhance the effectiveness of seeding, it is important to examine the relationships between seeding conditions and the properties of the obtained polymorphs. A review on seeding in polymorphic crystallization is available.<sup>1</sup> For instance, in the manufacturing of abecanil<sup>2</sup> and ritonabil,<sup>3</sup> crystallization has been controlled by using seed crystals of desired polymorphs.

In our recent study<sup>4</sup> using 4-(1-(2-(3-methoxyphenethyl)phenoxy)-3-(dimethylamino)propan-2-yloxy)-4-oxobutanoic acid (MPP0), which possesses two polymorphs (Form A and Form B), because the solubility difference between the two polymorphs in aqueous 2-butanone was found to be quite small, polymorphic mixtures were produced from batch crystallization with mixed seeds. Because the solubilities of the two polymorphs were nearly identical, it is unlikely that solution-mediated transformation occurred for this system. Among the operating variables examined, the polymorphic seed composition and supersaturation at the moment of seeding were found to determine the polymorphic composition of the product particles. In the experiments, the seeds were prepared by milling both polymorphic particles and mixing them together. Prior to mixing, they had broad but identical size distributions with a

median size of about 10  $\mu\text{m}$ . By analyzing the size and polymorph distributions of the product, it was found that the median particle size of Form A was consistently smaller than that of Form B. Therefore, it was concluded that the growth rate of Form B was faster than that of Form A.

If the kinetics of nucleation and growth of both polymorphs are different, the seed size may influence the polymorphic composition of the product. For example, since smaller seeds have larger surface areas, the mass deposition rate, which would be proportional to the surface area, would generally be faster than that for larger seeds. This means that the consumption of the supersaturation is faster for smaller seeds compared with larger seeds if the same amount was fed. In addition, the frequency of breakage by agitation may be higher for large crystals than for small crystals. This effect may be greatly enhanced when the polymorphs exhibit different crystallization behaviors.

In the present study, the above idea is examined for the MPP0-aqueous 2-butanone mixed solvent system using well-defined classified particles as seeds to clarify the effects of seed size and different crystallization behaviors between the polymorphs on the polymorphic composition and size distribution of the product.

## 2. Experimental Methods and Procedures

**2.1. Materials Used in Experiment.** MPP0 was obtained from Ohara Pharmaceutical Co., Ltd. Its chemical purity as analyzed by HPLC was >99%, and impurities in excess of 0.1% were not detected. 2-butanone (Nacalai Tesque, Inc., gas chromatographic purity >98%) and distilled water (Wako Pure Chemical Industries, Ltd.) were used as received. Polymorphic purities were determined by the method of powder X-ray diffraction (PXRD) analysis with  $\text{CuK}\alpha$  radiation at 40 mA and 45 kV (Bruker Model Discover with GADDS), infrared absorption spectrometry (Shimadzu FTIR 8400), and differential scanning calorimetry (Netzsch DSC 204 F1). Polymorphic compositions were determined by PXRD.

For the calculation of volume shape factors, the crystal density of both polymorphs was measured by an immersion method (measured temperature: 295–296 K) using isopropyl-ether (Nacalai Tesque, Inc., gas chromatographic purity >98%).

**2.2. Solubility and Polymorphic Compositions.** The solubility data for the two polymorphs in aqueous 2-butanone solutions reported in a previous study<sup>4</sup> were used. They were correlated by the following empirical equation:

$$x = \exp\left(A + \frac{B}{T} + C \ln T\right) \quad (1)$$

\* To whom correspondence may be sent. E-mail: yoshitaka@ohara-ch.co.jp.

† OHARA Pharmaceutical Co.

‡ Tokyo University of Agriculture and Technology.

- (1) Beckmann, W. *Org. Process Res. Dev.* **2000**, *4*, 372.
- (2) Chemburkar, S. R.; Bauer, J.; Deming, K.; Spiwek, H.; Patel, K.; Morris, J.; Henry, R.; Spanton, S.; Dziki, W.; Porter, W.; Quick, J.; Bauer, P.; Donaubaer, J.; Narayanan, B. A.; Soldani, M.; McFarland, K. *Org. Process Res. Dev.* **2000**, *4*, 413.
- (3) Beckmann, W.; Nickisch, K.; Buddle, U. *Org. Process Res. Dev.* **1998**, *2*, 298.
- (4) Nakata, Y.; Kiyosawa, Y.; Kagara, K.; Matsuoka, M. *Org. Process Res. Dev.* **2009**, *13*, 1364.

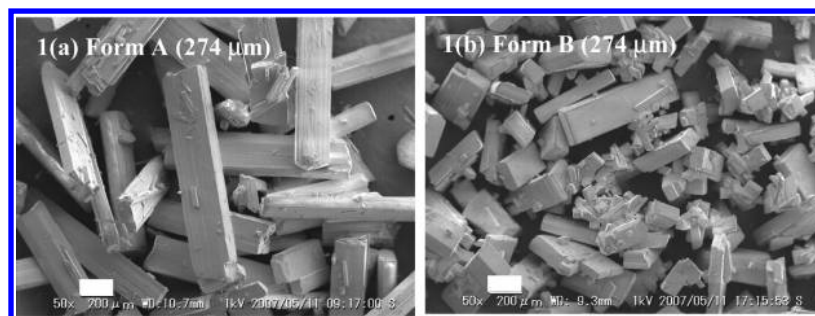


**Figure 1.** SEM images of Form A (a) and Form B (b) for seed particles of  $L_s = 274 \mu\text{m}$ . Scale:  $200 \mu\text{m}$ .

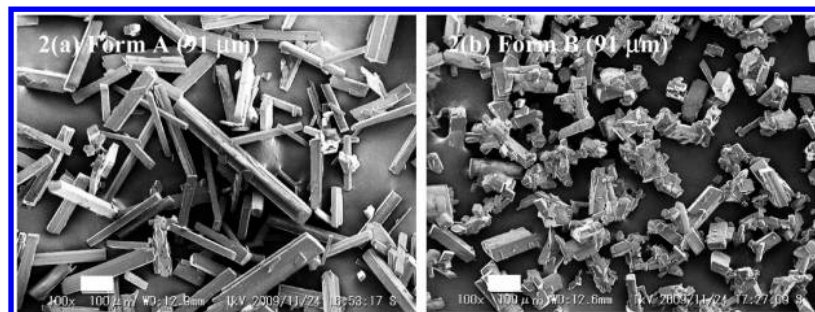


**Figure 2.** SEM images of Form A (a) and Form B (b) for seed particles of  $L_s = 91 \mu\text{m}$ . Scale:  $100 \mu\text{m}$ .

where the values of the constants  $A$ ,  $B$ , and  $C$  were reported<sup>4</sup> as a function of solvent composition ( $w$ ). In the crystallization, Form B was initially the metastable form until the addition of the poor solvent; however, it is stable at the final temperature (293 K) because the transition temperature of  $w = 0.073$  and  $0.037$  is 317 K and 332 K, respectively.<sup>4</sup> In our preliminary experiments, polymorphic transformation did not occur in solutions or in the solid in the temperature range covering the transition temperatures.

The polymorphic composition ( $X_A$ ) was determined from the characteristic peaks of Form A at  $2\theta = 10.3^\circ$  and  $11.1^\circ$  and the peak of Form B at  $2\theta = 10.7^\circ$ , through a calibration curve prepared in advance.<sup>4</sup>  $X_{Ap}$  and  $X_{As}$  denote the polymorphic composition of the product and the seed, respectively.

**2.3. Crystallization Procedure.** A 2 L glass vessel (inner diameter of 14 cm and depth of 15 cm) was used as the crystallizer. It was equipped with a jacket, a three-blade retreat agitator 90 mm in diameter, and a beaver-tail baffle. To prepare a mother liquor, 150 g of MPPO was dissolved in 619 g of aqueous 2-butanone solution (water content in mass fraction,  $w = 0.073$ ) at 348 K and was stirred at 215 rpm. The saturation temperature of this solution was 338 K. After complete dissolution, it was cooled to 323 K in about 25 min.

When the solution temperature reached 323 K, 1.5 g of seed crystals was added, the amount corresponding to 1.0 mass % of the dissolved MPPO. After seeding, the solution was maintained at the same temperature for 1 h. Subsequently, 589 g of a second solvent—2-butanone at 323 K—was added in about 1 min to reduce the solubility. This led the solvent composition to become  $w = 0.037$ . The solution was then kept for another 30 min at the same temperature and was again cooled down to 293 K in about 30 min.

After this solution was maintained at 293 K for 1 h, the product particles were taken out and dried. They were divided into two parts of approximately 70 g each. One half was milled by a cutter mill (Wonder Crush/Mill, D3 V-10) to measure the

mean polymorphic composition ( $X_{Ap}$ ). The rest was used to measure the particle size distribution using a sieve shaker (NITTO ANF-30). On the basis of these data, the polymorphic composition distribution was determined.

**2.4. Preparation of Seeds and Measurement of Particle Size Distribution.** Pure crystals of Form A and Form B were prepared from aqueous 2-butanone and aqueous acetone solutions, respectively.<sup>4</sup> They were sieved separately and then mixed to prepare a polymorphic seed having a composition of  $X_{As} = 0.90$  in the mass fraction of Form A.

The seed size ranged from 91 to  $274 \mu\text{m}$ . Figures 1 and 2 show typical SEM images of classified crystals of both polymorphs. The particles in Figure 1 are the largest seeds, while those in Figure 2 are smallest.

The particle size distribution of the product was measured by sieving with standard sieves whose openings ranged from 53 to  $710 \mu\text{m}$ . The mass of crystals ( $\Delta W$ ) on each sieve was measured and was divided by the difference ( $L_1 - L_2 = \Delta L$ ) between successive sieve openings ( $L_1$  and  $L_2$ ). The obtained values of  $\Delta W/\Delta L$  were plotted against the arithmetic median particle size ( $L = (L_1 + L_2)/2$ ). The particle size at the cumulative mass fraction of 0.50 was defined as the median particle size of the product,  $L_p$ . To calculate the coefficient of variation (CV), the sizes at cumulative mass fractions of 0.841 and 0.159, respectively, were used in addition to  $L_p$ .

**2.5. Volume Shape Factor of Both Polymorphs.** Using particle size  $L$ , the volume shape factor ( $\Phi_v$ ) defined by  $\Phi_v = W/(n\rho_s L^3)$  was calculated, where  $\rho_s$  is the crystal density,  $n$  is the number of crystals of size  $L$ , and  $W$  is the mass of the  $n$  crystals. Volume shape factors for both polymorphs ( $\Phi_{vA}$ ,  $\Phi_{vB}$ ) of various particle sizes (91, 137, 163, 214, 274, 326, 390,  $550 \mu\text{m}$ ) were calculated, and their ratios ( $\Phi_{vA/B} = \Phi_{vA}/\Phi_{vB}$ ) were determined. The number of crystals ( $n$ ) was counted twice under a microscope, and the average value was used to calculate the volume shape factor. The actual particle number was between

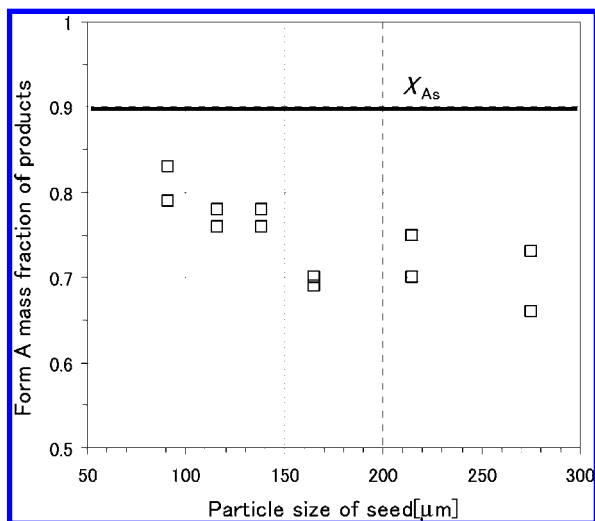


**Figure 3.** Effect of seed size on polymorphic composition of products with seed composition ( $X_{As}$ ) of 0.90.

300 and 500. For particles 91  $\mu\text{m}$  in size, about 1200 particles were counted using SEM images of which mass was measured.

### 3. Results and Discussion

**3.1. Variation of Polymorphic Compositions with Seed Size.** With a seed of  $X_{As} = 0.90$ , the product composition ( $X_{Ap}$ ) was found to be consistently lower than  $X_{As}$  and varied with the seed size. As shown in Figure 3, larger seeds showed a tendency to lead to lower compositions. The observation  $X_{Ap} < X_{As}$  is in good agreement with previous findings.<sup>4</sup> The difference between  $X_{Ap}$  and  $X_{As}$ , as well as the variation in  $X_{Ap}$  with the seed size, are likely to have been caused by the different crystallization behaviors between the polymorphs.

**3.2. Crystallization Behaviors of Polymorphs.** To understand the nucleation and growth behaviors of both polymorphs, crystallizations using pure polymorphic seeds were carried out with a seed size of 91  $\mu\text{m}$ . The crystallization procedure was the same as that described in section 2.3, with the exception of the usage of pure seeds.

The product particles of both polymorphs showed broad size distributions, as shown in Figure 4a for Form A and Figure 4b for Form B. They were different in median size as well as in the distribution pattern. The median size was 260  $\mu\text{m}$  for Form A and 375  $\mu\text{m}$  for Form B, and the CV values were 77% and 45%, respectively. These results indicate that Form B is clearly larger than Form A and that Form B has a narrower distribution. The results show different kinetics of nucleation, growth, agglomeration, and breakage between the polymorphs.

Table 1 shows that the values of the volume shape factors of both polymorphs varied substantially with particle size. In the calculations, the values of the densities of 1.29  $\text{g}/\text{cm}^3$  and 1.30  $\text{g}/\text{cm}^3$  were used for Form A and Form B, respectively. Although there are large variations in the values of individual shape factors, the ratio shows a general pattern in which its value is rather close to unity for particles larger than 274  $\mu\text{m}$  and larger than unity for particles smaller than this size.

The volume shape factor value for Form A at 163  $\mu\text{m}$  is exceptionally high, indicating elongated shapes. As shown in Figure 5a, many Form A crystals possess a length of about 1 mm and high aspect ratios; therefore, the volume shape factor

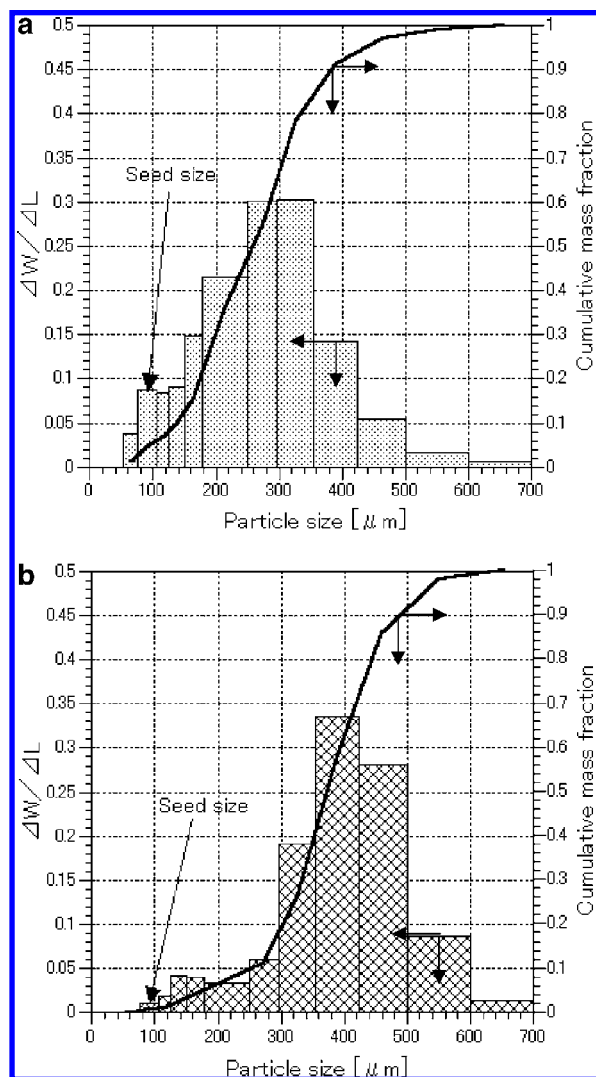


**Figure 4.** (a) Particle size distribution of Form A,  $L_s = 91 \mu\text{m}$ . The arrows indicate the referred axis. (b) Particle size distribution of Form B,  $L_s = 91 \mu\text{m}$ .

**Table 1.** Volume shape factors of both polymorphs;  $\Phi_{vA}$ ,  $\Phi_{vB}$  = volume shape factors of Form A and Form B, respectively;  $\Phi_{v, A/B} = \Phi_{vA}/\Phi_{vB}$

median particle size ( $\mu\text{m}$ )	volume shape factor		ratio
	$\Phi_{vA}$	$\Phi_{vB}$	$\Phi_{v, A/B}$
91	1.27	0.89	1.43
137	2.03	1.40	1.45
163	2.93	1.29	2.27
214	1.38	1.12	1.23
274	0.93	0.93	1.00
326	1.00	1.25	0.80
390	0.60	0.78	0.77
550	0.39	0.44	0.89

is quite large. Meanwhile, Form B crystals of the same size are much shorter (Figure 5b), resulting in a smaller volume shape factor than that for Form A. For Form A particles smaller than 163  $\mu\text{m}$  the factor becomes smaller again, and this may probably have arisen from the breakage of larger particles. The lengths are unevenly distributed, and some broken crystals are observed in the Form A crystal 91  $\mu\text{m}$  in size (Figure 6a). However, as shown in Figures 5b, 6b, and 7b, some Form B



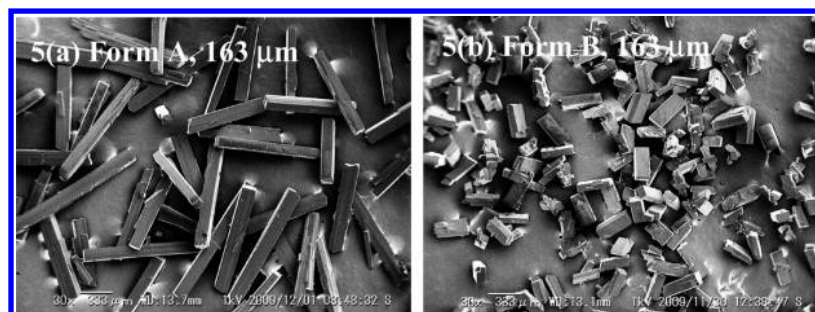


Figure 5. Classified particles of  $L = 163 \mu\text{m}$ . (a) Form A:  $\Phi_{vA} = 2.93$ , and (b) Form B:  $\Phi_{vB} = 1.29$ . Scale:  $333 \mu\text{m}$ .

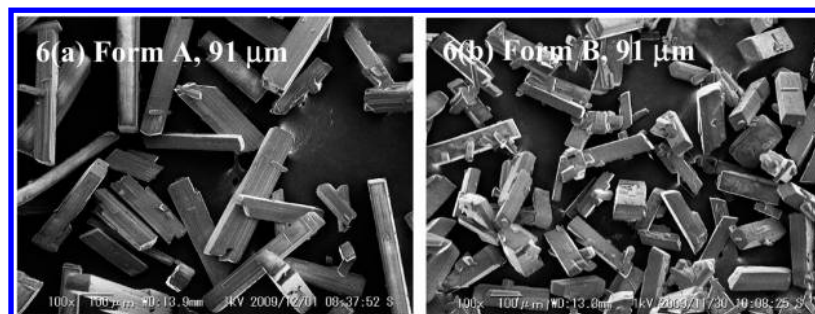


Figure 6. Classified particles of  $L = 91 \mu\text{m}$ . (a) Form A:  $\Phi_{vA} = 1.27$ , and (b) Form B:  $\Phi_{vB} = 0.89$ . Scale:  $100 \mu\text{m}$ .

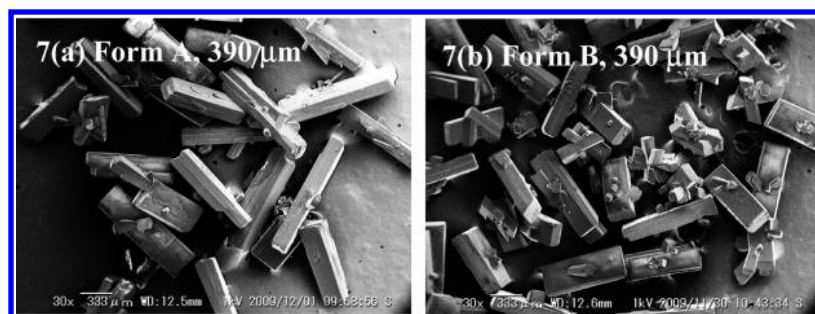


Figure 7. Classified particles of  $L = 390 \mu\text{m}$ . (a) Form A:  $\Phi_{vA} = 0.60$ , and (b) Form B:  $\Phi_{vB} = 0.78$ . Scale:  $333 \mu\text{m}$ .

crystals are agglomerated, and their shape is platelike and almost independent of size.

As the particle size increases, (see images a and b of Figure 7), the shapes of both polymorphs become similar, and the width of Form A crystals is broadened. Therefore, their volume shape factors approached unity.

### 3.3. Crystallization Behaviors of Polymorphic Mixtures.

Using a mixed seed of  $X_{As} = 0.90$ , the polymorphic composition and size distributions of the product were analyzed to understand the difference in growth behaviors between the polymorphs. For this purpose, two seed sizes were used. Figure 8a shows, in the case of large seeds ( $L_s = 274 \mu\text{m}$ ), the product size distribution and its cumulative curve, as well as the polymorphic composition distribution as a function of particle size. The polymorphic composition showed significant dependence on particle size. Although  $X_{Ap} = 0.66$  in this case, the composition was not constant over the entire size range but showed variations around the mean value. The fact that about 70 mass % of the product was smaller than the seed leads to the conclusion that substantial nucleation and breakage has occurred during crystallization.

A similar analysis was carried out in the case of small seeds ( $L_s = 91 \mu\text{m}$ ). As already shown in Figure 3, smaller seeds tend to produce relatively higher compositions of Form A compared with the larger seed. Figure 8b shows, for the case of small seeds, a very distinct distribution of polymorphic compositions, for which the mean product composition was  $X_{Ap} = 0.84$ . It can be clearly observed that the polymorphic composition of particles smaller than  $250 \mu\text{m}$  was almost always  $X_A = 0.90$  or higher, whereas that of particles larger than  $300 \mu\text{m}$  was definitely far lower. This suggests that Form B grew much faster than Form A.

It may be interesting to note that if the crystallization kinetics are independent of each other during crystallization, the curve in Figure 8b may be the summation of 90% Form A (Figure 4a) and 10% Form B (Figure 4b). This was not actually the case since the consumption of supersaturation was different between the polymorphs. This indicates that the crystallization behavior differed between polymorphs. In addition, agglomeration might have played a role in this size distribution, particularly for Form B.

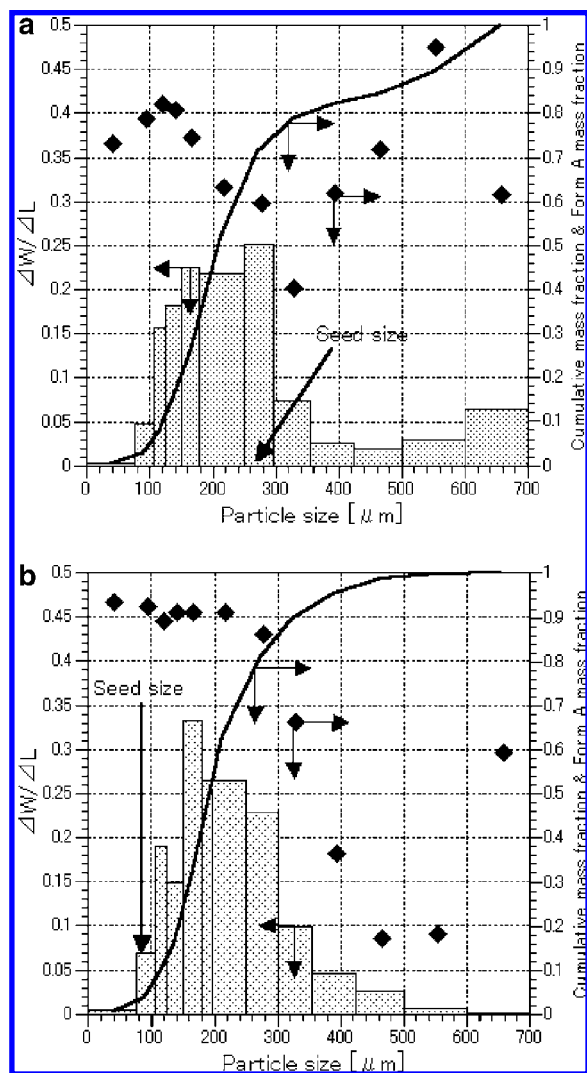


**Figure 8.** (a) Distributions of particle size and polymorphic composition,  $L_s = 274 \mu\text{m}$ ,  $X_{As} = 0.90$  (b) Distributions of particle size and polymorphic composition,  $L_s = 91 \mu\text{m}$ ,  $X_{As} = 0.90$ .

To highlight the different crystallization behaviors between the two polymorphs, size distributions of each polymorph were constructed to reveal how the distributions in the product varied when seeds of different size were used. The size distributions of each polymorph were calculated from the data on the distributions of product size and polymorphic composition.

Figures 9a and 9b show comparisons of the calculated cumulative mass fractions undersize of both polymorphs for six seed sizes. It is clear that in the case of the largest seed ( $274 \mu\text{m}$ ), the median size of Form A of the product ( $L_p = 200 \mu\text{m}$ ) is smaller than that of Form B ( $L_p = 230 \mu\text{m}$ ) and that these two values are definitely smaller than the seed size ( $L_s = 274 \mu\text{m}$ ). As mentioned above, the mean polymorphic composition was  $X_{Ap} = 0.66$  although  $X_{As} = 0.90$ , indicating that the mass of Form B deposition was larger than that of Form A deposition. These findings imply that in addition to the faster growth of Form B its nucleation also occurred more easily than that of Form A.

In the case of the smallest seed ( $L_s = 91 \mu\text{m}$ ), the median sizes of Form A and Form B were  $L_p = 190 \mu\text{m}$  and  $L_p = 290$

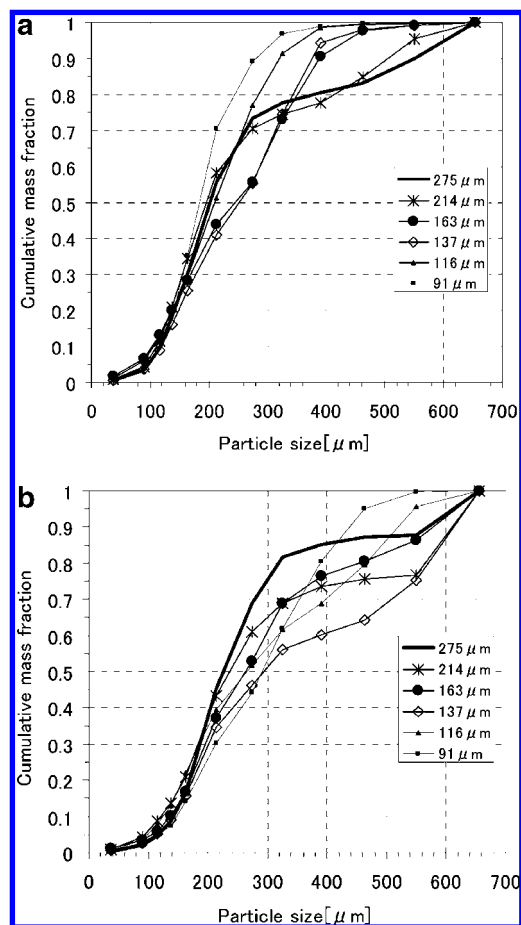


**Figure 9.** (a) Effect of seed size on particle size distributions for Form A. (b) Effect of seed size on particle size distributions for Form B.

$\mu\text{m}$ , both of which were larger than the seed size by a factor of about 2 and 3, respectively. While this indicates that they did grow, their nucleation behaviors are not clear.

Furthermore, in cases of larger seeds ( $L_s = 214$  and  $274 \mu\text{m}$ ), the median sizes were smaller than the seed size, and their distributions also had shoulders resulting from nucleation and breakage during crystallization. Smaller seeds, on the contrary, had sharper and monodispersed distributions, implying less nucleation and breakage. These findings were common to both polymorphs.

#### 4. Conclusions

To clarify the effect of seed size on the distribution of particle sizes and polymorphic compositions of products, batch cooling and drowning-out crystallization experiments were carried out using MPPO which has two polymorphs of Form A and Form B. The mean polymorphic composition of Form A of the product approached that of the seed as the seed size decreased, although it was always lower than the seed composition. The higher composition of Form B was explained by the faster crystallization of Form B than that of Form A. The volume shape factors of both polymorphs varied with size, but their ratio neared unity as the size increased.

The particle size distributions of both polymorphs were broad, showing the occurrence of nucleation, growth, breakage,

and agglomeration during crystallization. The particle size distribution of both polymorphs became bimodal as the seed became larger, indicating that secondary nucleation of both polymorphs occurred. From the size and composition distributions, it is concluded that Form B grows faster and nucleates more easily than Form A.

### Acknowledgment

We express our deepest gratitude to the members of the fine chemical group, OHARA Pharmaceutical Co., Ltd., for their useful advice and kind support. This study was partially supported by a Grant-in-Aid for Scientific Research (B) from the Japan Society for the promotion of Sciences (JSPS).

### Nomenclature

<i>A</i>	constant in eq 1
<i>B</i>	constant in eq 1
<i>C</i>	constant in eq 1

<i>x</i>	solubility in mole fraction
<i>T</i>	absolute temperature
<i>L</i>	size
<i>W</i>	mass of crystal on sieve
<i>w</i>	water content in solvent in mass fraction
<i>X<sub>A</sub></i>	mass fraction of Form A
$\Phi_{vA}, \Phi_{vB}$	volume shape factors of Form A and Form B, respectively
$\Phi_{v,A/B}$	ratio of volume shape factors

### Superscripts and Subscripts

p	product
s	seed or seeding

Received for review November 4, 2009.

OP900289U